research articles Journal of proteome research

New Candidate Targets of AMP-Activated Protein Kinase in Murine Brain Revealed by a Novel Multidimensional Substrate-Screen for Protein Kinases

Roland D. Tuerk,[†] Ramon F. Thali,[†] Yolanda Auchli,[‡] Helene Rechsteiner,[⊥] René A. Brunisholz,[‡] Uwe Schlattner,[#] Theo Wallimann,[†] and Dietbert Neumann*,[†]

Institutes of Cell Biology and Molecular Biology & Biophysics, ETH Zurich, 8093 Zurich, Switzerland, Functional Genomics Center Zurich (FGCZ), University of Zurich, 8057 Zurich, Switzerland, and Laboratoire de Bioénergetique Fondamentale et Appliquée, INSERM, U884, Université Joseph Fourier BP 53, 38041 Grenoble cedex 9, France

Received March 21, 2007

AMP-activated protein kinase (AMPK) is a heterotrimeric serine/threonine kinase that is involved in the maintenance of energy homeostasis and recovery from metabolic stresses both at the cellular and whole body level. AMPK is found in all tissues examined so far, and a number of downstream targets have been identified. Recent work suggests that AMPK has specialized functions in the brain, such as involvement in appetite control. Nevertheless, brain-specific substrates of AMPK are unknown. Here, we performed a proteomic *in vitro* screen to identify new putative AMPK targets in brain. Prefractionation of murine brain lysates by liquid chromatography, utilizing four different, serially connected columns with different chemistries was found to be superior to a single column method. A pilot screen involving incubation of small volumes of individual fractions with radiolabeled ATP in the presence or absence of active AMPK, followed by one-dimensional SDS-PAGE and autoradiography, revealed the presence of potential AMPK substrates in a number of different fractions. On the basis of these results, several kinase assays were repeated with selected fractions on a preparative scale. Following separation of the radiolabeled proteins by two-dimensional electrophoresis and comparison of samples with or without added AMPK by differential autoradiography, 53 AMPK-specific phospho-spots were detected and excised. Thereof, 26 unique proteins were identified by mass spectrometry and were considered as new potential downstream targets of AMPK. Kinase assays with 14 highly purified candidate substrate proteins confirmed that at least 12 were direct targets of AMPK *in vitro*. Although the physiological consequences of these phosphorylation events remain to be established, hypotheses concerning the most intriguing potential targets of AMPK that have been identified by this search are discussed herein. Our data suggests that signaling by AMPK in brain is likely to be involved in the regulation of pathways that have not yet been linked to this kinase.

Keywords: AMP-activated protein kinase • phosphorylation • multidimensional separation • liquid chromatography • two-dimensional electrophoresis • phosphoproteomics • MALDI • mass spectrometry • multidimensional substrate-screen for protein kinases • MudSeek

Introduction

A fundamental process in all living cells is the monitoring and maintenance of cellular energy pools. The AMP-activated protein kinase (AMPK) cascade works as a key sensor and regulator of energy balance at the cellular and whole body level. AMPK is a heterotrimeric Ser/Thr kinase comprising a catalytic α-subunit and regulatory β- and γ-subunits.[1] It is activated by a variety of physiological and pathological stresses, for example, by exercise, glucose deprivation, ischemia, or hypoxia.[2] Activation of AMPK occurs primarily through phosphorylation at Thr-172 of the catalytic α-subunit by the tumor suppressor LKB1 or by CaMKKβ.[3−6] Furthermore, it is allosterically activated by an increasing AMP/ATP ratio as a consequence of metabolic stresses that deplete ATP-levels.[7,8] Once activated, AMPK inhibits biosynthetic processes that consume ATP such as protein synthesis, gluconeogenesis, or synthesis of fatty acids and glycogen. Simultaneously, active AMPK stimulates pathways that generate ATP, like glucose uptake, glycolysis, or fatty acid oxidation to restore cellular ATP levels.[9]

* To whom correspondence should be addressed. Institute of Cell Biology, ETH Zurich, Schafmattstrasse 18, HPM D23, CH-8093 Zurich, Switzerland, Tel.: +41 (0)44 633 33 91. Fax: +41 (0)44 633 10 69. E-mail: dietbert.neumann@cell.biol.ethz.ch.

[†] Institute of Cell Biology, ETH Zurich.

[⊥] Institute of Molecular Biology & Biophysics, ETH Zurich.

[‡] Functional Genomics Center Zurich.

[#] Université Joseph Fourier and INSERM.

10.1021/pr070160a CCC: $37.00
Published on Web 07/04/2007

Research during the last decades so far revealed 20 proteins that are phosphorylated and regulated by AMPK *in vivo*.[10−15] Many of these targets were initially discovered in cultured cells, and physiological significance has been shown mainly in liver, skeletal muscle, heart, or adipose tissue. Indeed, the role of AMPK in these particular tissues involved in type-2 diabetes mellitus (T2DM) is currently under extensive investigation, also motivated by the discovery of AMPK activation by Metformin, a widely used drug for treatment of T2DM.[16] In particular, there is strong evidence that increased glucose uptake in skeletal muscle by administration of Metformin is mediated by AMPK.[17] Most importantly, there is good evidence that AMPK activation in liver is the main mechanism for the blood glucose lowering effect of the drug.[17,18] In adipocytes, AMPK inhibits lypolysis by phosphorylation of hormone-sensitive lipase,[19] thereby lowering circulating free fatty acid levels.

Contrary to the studies in peripheral tissues, relatively little is known about AMPK in brain.[20] Although AMPK was found throughout this organ,[21,22] most studies focused on its role in the hypothalamus as a sensor and regulator of whole body energy status.[23] Much interest in this field derived from findings that hypothalamic AMPK activity is regulated by anorexigenic and orexigenic hormones such as leptin or ghrelin.[24−26] However, the up- and downstream players in the hypothalamic AMPK cascade mediating the actions of these hormones are largely unknown. Besides its function in the hypothalamus, it was reported that activation of AMPK is cytoprotective for neurons following chemical hypoxia or glucose deprivation.[21] Controversially, other studies support the notion that inhibition of AMPK exerts anti-apoptotic effects under conditions of oxidative stress or ischemia.[27,28] Obviously, further studies investigating the role of AMPK in brain are needed to elucidate its poorly defined function in the various specialized cells of this tissue, which likely involves hitherto unknown downstream targets of AMPK.

To shed new light into AMPK signaling in brain, we aimed at the discovery of novel candidate targets of this kinase and, therefore, developed a proteomic screening approach. Proteins from murine whole brain extracts were separated and selectively enriched by chromatography with four different columns working by differing separation principles were connected in series. The fractions were subjected to kinase assays with recombinant active AMPK in the presence of [γ-^{32}P]ATP, followed by 2-DE and autoradiography. We detected 53 spots on the autoradiographs resulting from AMPK-specific incorporation of radiolabeled phosphate and identified 26 novel candidate substrates by mass spectrometry. Thereof, 14 highly purified candidate proteins were tested, and 12 were confirmed as *in vitro* substrates of AMPK. The method should be generally applicable for any protein kinase and tissue and was therefore termed MudSeeK (*mu*lti*d*imensional *s*ubstrate-scr*ee*n for protein *k*inases).

Experimental Section

Materials. [γ-^{32}P]ATP was purchased from Hartmann Analytic (Braunschweig, Germany). IPG buffer, strips, and Ettan IPGphor II isoelectric focusing unit were from GE Healthcare (Otelfingen, Switzerland). CRMP2 was purchased from Kinasource, Ltd. (Dundee, Scotland, U.K.). Peptide calibrant standard II (#222570), α-cyano-4-hydroxy-cinnamic acid (CHCA), MTP 384 massive MALDI target (gold plated, #26993), and the Ultraflex TOF/TOF II MALDI mass spectrometer were from Bruker Daltonics (Bremen, Germany). ZipTip C18 microcolumns were purchased from Millipore (Zug, Switzerland). TPP2 was obtained from Biomol (Hamburg, Germany). β-Synuclein was from Chemicon International (Hampshire, U.K.). PACSIN1 was a generous gift from Dr. M. Plomann (University of Cologne, Cologne, Germany). Tubulin, α-actin, and β/γ-actin were purchased from Cytoskeleton, Inc. (Denver, CO). Citrate synthase, glutamate dehydrogenase, and GAPDH were obtained from Roche Applied Science (Rotkreuz, Switzerland). Prostaglandin E2 synthase (p23) was a kind gift from Prof. D. Toft (Mayo Clinic College of Medicine, Rochester, NY). GFAP was purchased from Calbiochem (San Diego, CA). Synapsin I was generously provided by Dr. Angus Nairn (Rockefeller University, NY). Hsc70 was purchased from Stressgen Bioreagents (Ann Arbor, MI). Plasmid pETHGS2 encoding human glutamine synthetase (GS) for expression in *Escherichia coli* was kindly provided by Dr. H. Morizono (Children's National Medical Center, Washington D.C.). To add an N-terminal His-tag, GS was subcloned into pET14bx using the NdeI/BlpI restriction sites,[29] resulting in pEThis-HGS2. The protein was expressed and purified essentially as described,[30] with the following modifications. The bacterial pellet was resuspended in modified GS buffer (10 mM potassium phosphate, pH 8.0). Following sonication, the lysate was centrifuged (40 min, 4 °C, 25 000*g*), and the supernatant was applied to a 5 mL HisTrap HP column (GE Healthcare, Otelfingen, Switzerland). The column was washed with 30 mL of GS buffer supplemented with 250 mM imidazole. Glutamine synthetase was eluted with 10 mL of GS buffer containing 750 mM imidazole and dialyzed against GS buffer supplemented with 5 mM DTT. Recombinant constitutively active AMPK $\alpha1\beta1\gamma1$ isoform containing an aspartic acid instead of a threonine at position 172 was expressed in *E. coli* and purified as published.[29,31]

Preparation of Murine Brain Extract. Total brains from 80 mice of mixed genetic background were snap-frozen in liquid nitrogen and homogenated with a Micro-Dismembrator S (Braun, Melsungen, Germany), yielding 54 mL of frozen powder. A volume of 15 mL powder was dissolved in 75 mL ice-cold extraction buffer (5 mM DTT, 100 mM NaCl, and 20 mM HEPES, pH 7.2) using a Polytron PT 3000 homogenizer (Kinematica, Littau, Switzerland) at 24 000 rpm for 20 s. The sample was further processed by applying three pulses of sonication (60% output, 10 s) with a Branson Sonifier 250 (VWR, Dietikon, Switzerland) followed by centrifugation at 100 000*g* for 2 h at 4 °C. The supernatant was desalted on a HiPrep 26/10 desalting column (GE Healthcare, Otelfingen, Switzerland) with buffer A (2 mM DTT and 10 mM HEPES, pH 7.2) or buffer B (2 mM DTT and 10 mM HEPES, pH 8.2) and filtered (through a 0.22 μm filter).

Prefractionation of Proteins by Strong Anion Exchange (SAX) Chromatography. Desalted brain extract (80 mg) in buffer B was applied to a SAX column (POROS HQ 20, 1.7 mL bed volume, Applied Biosystems, Rotkreuz, Switzerland) preequilibrated in buffer B. The column was then washed at a flow rate of 1 mL/min with 10 mL of buffer B, developed with a linear gradient for 38 min from 0 to 1 M NaCl in buffer B, and fractions of 1 mL were collected.

Prefractionation of Proteins by Chromatography with Serially Stacked Columns. Four HiTrap HP columns (1 mL bed volume, GE Healthcare, Otelfingen, Switzerland) were connected in series in the following order (top to bottom): Heparin Sepharose, Blue Sepharose, SP Sepharose (strong cation exchanger), Q Sepharose (strong anion exchanger) and preequilibrated in buffer A. Desalted brain extract (50 mg) in buffer

A was applied on top of the stack at a flow rate of 0.5 mL/min, followed by a washing step for 40 min with buffer A. The first 8 mL of the flow-through were collected. The serially stacked columns were disconnected, and proteins were eluted separately from each column by a stepwise NaCl gradient (10 mM, 50 mM, 200 mM, 1 M, and 2 M) in buffer A for 5 mL each. Proteins from the Blue Sepharose column were eluted with 5 mL of a nucleotide buffer (15 mM NADH, 15 mM NADPH, 20 mM AMP, 20 mM ATP, 5 mM DTT, and 100 mM HEPES, pH 7.2) prior to elution with salt. Fractions of 1 mL were collected throughout the procedure.

1-D Screening for AMPK Substrates. AMPK assays were performed with 20 μL of various fractions (see Figure 3B) by incubation with or without recombinant constitutively active AMPK (60 pmol) at 37 °C in kinase buffer (200 μM [γ-^{32}P]ATP with a specific activity of 400 mCi/mmol ATP, 50 μM AMP, 5 mM $MgCl_2$, 1 mM DTT, and 10 mM HEPES, pH 7.2) at a final volume of 40 μL. The kinase reactions were then stopped exactly after 1 min by addition of 10 μL of SDS sample buffer (105 mM Tris-HCl, pH 6.8, 4% (w/v) SDS, 15% (v/v) glycerol, 1.2 M 2-mercaptoethanol, and 0.02% (w/v) bromophenol blue), heated to 95 °C for 5 min, and separated by SDS-PAGE using large 12% gels (220 mm length, CBS Scientific Co., Del Mar, CA). Following colloidal Coomassie staining,[32] gels were air-dried between two layers of cellophane and exposed to Biomax MR autoradiography films (Kodak SA, Renens, Switzerland) for up to 2 weeks to reveal potential substrates of AMPK.

2-D Screening for AMPK Substrates. Between 300−600 μg of six fractions (flow-through, Heparin Sepharose 19−21, Q Sepharose 21, SP Sepharose 20) were incubated at 37 °C with or without AMPK (100 pmol) in kinase buffer at a volume of 290 μL. To stop the reactions after 1 min, the mixtures were transferred to new tubes containing 100 mg of urea, 7 mg of CHAPS, and 7 μL of a DTT stock (1 M) yielding a final concentration of 4.76 M urea, 2% (w/v) CHAPS, and 20 mM DTT at a resulting volume of 350 μL. The samples were vortexed frequently for 15 min and dialyzed against 1 L of freshly prepared 2-D sample buffer (7 M urea, 2 M thiourea, and 10 mM DTT) for 10−12 h at 20 °C. After addition of 0.5% (v/v) IPG buffer, 2% (w/v) CHAPS, and 0.002% (w/v) bromophenol blue, samples were applied to IPG strips (18 cm, pH 3−10). In-gel rehydration and 2-DE were performed using the Ettan IPGphor II unit as published,[33] except that 12% polyacrylamide gels were used for the second dimension. Colloidal Coomassie staining, gel drying, and autoradiography were performed as described above.

Trypsin Digestion and Mass Spectrometry. After development, the autoradiography films were realigned to the dried 2-D gels. Radioactively labeled spots in the gel were marked by piercing with a razor blade through film and gel at the position of AMPK-specific signals. Consequently, the spots on the 2-D gels, corresponding to the signals of interest, were clearly located and marked for later spot excision. To avoid contamination by keratin and dust particles, the following procedures, including in-gel digestion, were performed in a laminar flow sterile bench. Dried gels were wiped with lint-free tissue paper soaked in methanol, and marked spots were cut out. After rehydration in water, the cellophane layers were removed, and the gel pieces were subjected to in-gel digestion with trypsin (Promega, Wallisellen, Switzerland) as described previously.[34] Extracted peptides were lyophilized and stored at −80 °C for 4−6 weeks to reduce radioactivity to non-critical levels. Peptides were reconstituted in 5 μL of 10% (v/v) acetonitrile (ACN) supplemented with 0.1% (v/v) trifluoracetic acid (TFA) and desalted using ZipTip C18 microcolumns as recommended by the manufacturer (Millipore). Peptides were eluted from the ZipTip in 3 μL of 50% (v/v) ACN/0.1% (v/v) TFA. An aliquot was mixed with an equal volume of α-cyano-hydroxy cinnamic acid (10 mg/mL in 50:50 ACN/water supplemented with 0.1% (v/v) TFA), spotted on a gold coated-MALDI target, and allowed to dry at room temperature. All spectra were obtained by MALDI MS and MALDI MS/MS using an Ultraflex TOF/TOF II equipped with the control and analysis software Compass v. 1.1 (Bruker Daltonics, Bremen, Germany). The mass spectrometer was operated in the positive ion reflector mode with 150 ns delayed extraction time; the nitrogen laser (337 nm) was set to a repetition rate of 50 Hz, and the ion acceleration voltage was 25 kV. Mass measurements were performed automatically through fuzzy logic-based software to accumulate 500−800 single laser shot spectra or manually to accumulate 2000 single laser shot spectra. All spectra were calibrated externally with the mass signals of the peptide calibrant standard II. Routinely, prior to automated acquisition, two spots were used for signal and parameter optimization. The first monoisotopic signals in the spectra were assigned automatically using the peak detection algorithm SNAP (Bruker Daltonics, Bremen, Germany). The smoothing algorithm of Savitzky-Golay was applied (width 0.2 m/z, cycle number 1). Processed MS and MS/MS spectra were combined using BioTools software (Bruker Daltonics, Bremen, Germany) to search the Uniref100 database (release 6.0), restricted to the taxonomy *Mus musculus,* using MASCOT software v. 2.0 (Matrix Science, London, U.K.). Mass errors of 150 ppm for both the peptide mass fingerprints and the precursor ions selected for fragmentation were allowed. A maximal tolerance of 0.2 Da was allowed for fragment ions. In addition, the search parameters tolerated both oxidation of methionine and carbamidomethylation of cysteine as variable modifications and included up to one missed cleavage for trypsin. Probability-based MOWSE scores greater than 63 were considered significant and not a random event ($p < 0.05$).[35]

***In Vitro* Verification of Potential Downstream Targets.** Highly purified candidate substrates (0.5−2 μg) of AMPK were incubated for 25 min at 37 °C in the presence or absence of 1 pmol of AMPK in kinase buffer. Kinase reactions were stopped by addition of SDS sample buffer and subjected to SDS-PAGE and autoradiography as described above. The stoichiometry of phosphorylation was determined in triplicate experiments as follows. Positively verified target proteins (3 μg) were incubated with heterotrimeric TD-AMPK (2 pmol) in kinase buffer (specific activity of 2000 mCi/mmol ATP) at 37 °C. Aliquots containing 500 ng of candidate targets were removed after 10, 30, 60, and 120 min of incubation, immediately mixed with SDS sample buffer, and separated by SDS-PAGE. Gels were Coomassie-stained and dried between two layers of cellophane, and bands corresponding to the target proteins were excised. The amount of ^{32}P-incorporation was measured by liquid scintillation counting and compared to a dilution series of radioactive kinase buffer to calculate the molar equivalent.

Results and Discussion

Identification of Downstream Candidate Targets of AMPK from Total Brain Lysates. Initial attempts to screen for potential downstream targets of AMPK were performed without prefractionation of the proteins. Murine brain extracts were simply centrifuged, and the soluble supernatant was incubated

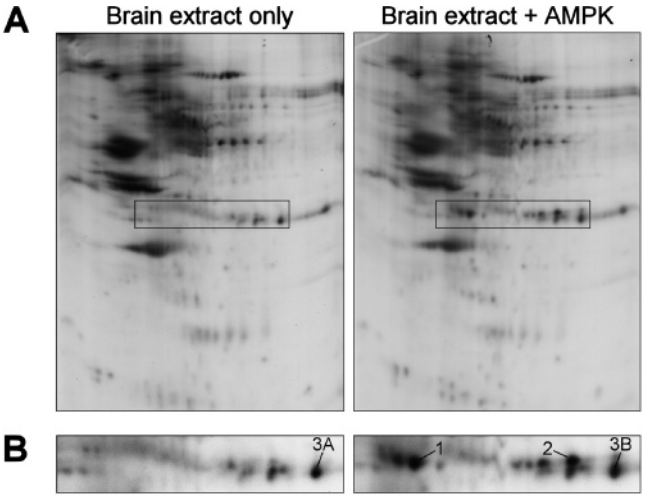

Figure 1. Autoradiograph showing potential downstream targets of AMPK detected in the nonfractionated brain extract. (A) A total of 400 μg of the desalted brain extract was directly incubated with [γ-^{32}P]ATP only (left panel) or together with an abundant amount of AMPK (right panel), followed by 2-DE and autoradiography. The positions and intensities of the spots caused by endogenous protein kinase activities were very reproducible, thereby allowing unambiguous detection of additional spots or changes in intensity emerging after addition of AMPK. (B) Magnification of the framed region in panel A. Only two additional spots (1 and 2) appeared after addition of AMPK, whereas spot 1 corresponded to the autophosphorylated β-subunit of AMPK itself. Spot 2 could not be identified with a significant score. Although equally labeled, spots 3A and 3B (glyceraldehyde-3-phosphate dehydrogenase) corresponded to abundant proteins on the gels and were analyzed to provide information about molecular weight and p*I* in this region.

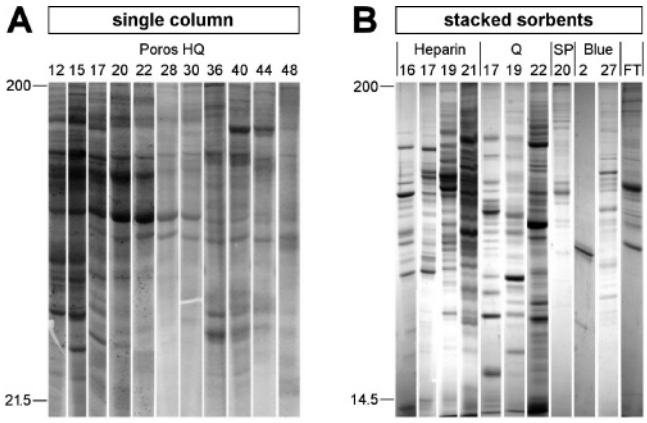

Figure 2. Chromatographic prefractionation of total brain extract. Proteins were either separated (A) by single anion exchange chromatography or (B) by chromatography with serially stacked sorbents, that were Heparin Sepharose (Heparin), Blue Sepharose (Blue), cation (SP) and anion (Q) exchange resins (in this order, top to bottom). The flow-through (FT) was collected, and proteins were subsequently eluted in parallel mode; i.e., the column stack was disassembled prior to elution. Samples of selected elution fractions were analyzed by SDS-PAGE followed by staining with Coomassie Blue. Fraction numbers are indicated on top of each lane. After single anion exchange chromatography, the fractions were still of high complexity, and many proteins were widespread over a number of fractions (A). In contrast, the stacked sorbents approach led to a very distinct band pattern even in adjacent fractions, indicating effective separation and enrichment of certain polypeptides in individual fractions (B).

with [γ-^{32}P]ATP either in the presence or absence of AMPK. After separation by 2-DE and autoradiography, the overall pattern of ^{32}P-labeled proteins appeared very similar, independently of whether AMPK was present in the fraction or not (Figure 1A). When the two autoradiographs were compared, the vast majority of proteins was labeled equally, likely reflecting mainly the action of endogenous kinases on their substrates in both assays. Nevertheless, only two additional radioactive spots were detected when AMPK was included in the assay (Figure 1B). These signals were considered AMPK-specific and, therefore, represent potential downstream targets with the precaution that AMPK also exhibits strong autophosphorylation of the α- and β-subunits.[36] Indeed, one of the spots was identified as the AMPK β-subunit (Figure 1B, spot 1). The identity of spot 2 (Figure 1B) could not be determined with a significant score (see Supporting Information Table S1), possibly due to the high complexity of the lysate causing multiple protein species to be present in this single spot. Because only one single spot disparate from AMPK subunits exhibited AMPK-specific incorporation of ^{32}P but was not identifiable by mass spectrometry, the kinase substrate screening method using whole brain lysates without prefractionation was inefficient, and further application was disregarded.

Chromatographic Prefractionation of Proteins. By two-dimensional electrophoresis, 1000−3000 proteins per gel can be visualized,[37] which is only a few percent of the total number of protein species present in a cell. Moreover, studies in yeast showed that low-abundance proteins make up 80% of the proteome,[38] underlining the necessity of prefractionation techniques to enrich and visualize these proteins. We investigated two different chromatographic strategies for prefractionation of desalted murine brain extract using (i) a single anion exchange column or (ii) four columns with different kinds of chemistries that were connected in series, that is, stacked on top of each other. While proteins from the single column were eluted by a linear salt gradient, the serially connected columns were disassembled, and each of the columns was developed individually by five incremental concentrations of sodium chloride. For the Blue Sepharose column, prior to stepwise salt elution, proteins were first eluted by application of a high concentration of nucleotides. Analysis of fractions by SDS-PAGE and Coomassie Blue-staining (Figure 2A) revealed a similar band pattern in adjacent fractions after chromatography by the single anion exchanger, suggesting that the same protein species were present in contiguous fractions. In addition, each of these fractions remained highly complex mixtures and still contained a large number of different polypeptide species. Hence, enrichment of single proteins, as reflected by strong bands in single fractions and lack of these bands in neighboring fractions, was not observed. Accordingly, we concluded that proteins in the brain extract were rather diluted to several fractions than efficiently separated and enriched by using a single anion exchange column for prefractionation. In contrast, the stacked sorbents approach virtually eliminated these redundancies as reflected by the distinct polypeptide band patterns obtained specifically with each of the different columns (Figure 2B). Furthermore, the fractions were of lower complexity and showed selective enrichment of various groups of proteins, which is expected to be beneficial for the visualization and identification of low-abundance proteins after one- and two-dimensional electrophoresis. Additionally, the stacked column approach was equally simple as chromatography by

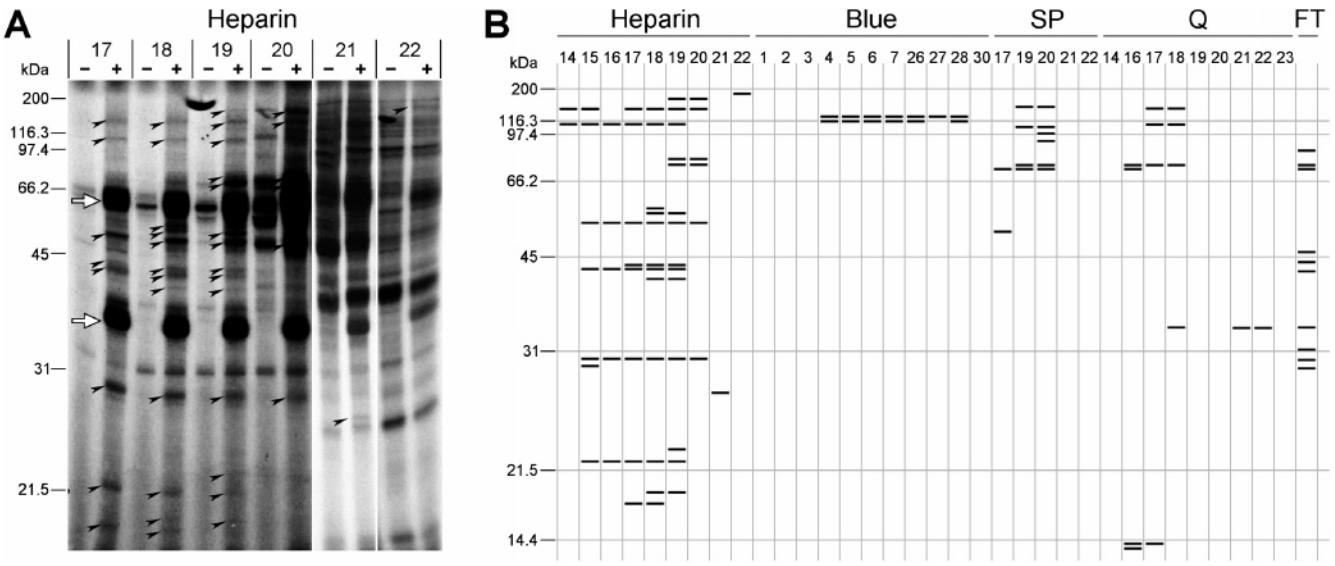

Figure 3. Detection of potential AMPK substrates in the prefractionated brain extract. (A) Representative autoradiograph of a 1-D screening assay with Heparin Sepharose fractions 17−22. Each fraction was incubated with [γ-^{32}P]ATP in the presence (+) or absence (-) of recombinant AMPK. The reaction mixtures were separated by SDS-PAGE, and phosphoproteins were detected by autoradiography. White arrows indicate strong autophosphorylation of the AMPK α- and β-subunits, whereas the black arrows point to proteins that were labeled only in presence of AMPK. Fractions 21 and 22 still contained a many different polypeptide species and exhibited a comparatively high background. For contrast adjustment, these autoradiographs were arranged separately. Fractions 17−20 revealed the vast majority of AMPK-specific ^{32}P-signals at different molecular weights. (B) Graphical representation of overall molecular weight distribution of polypeptides showing AMPK-specific labeling throughout the 35 fractions used in the kinase assays. Heparin, Heparin Sepharose; Blue, Blue Sepharose; SP, cation exchanger; Q, anion exchanger; FT, flow-through.

the single column without significantly increasing the number of fractions. Therefore, the fractions from the former approach were chosen for the one-dimensional "pilot screen" for AMPK substrates. On the basis of the results of this pre-screening, the most promising fractions were then selected for a final two-dimensional substrate-screen at preparative scale.

1-D Screen for AMPK Substrates. Only a subset of fractions derived from chromatography by the serially stacked sorbents approach was screened for putative downstream targets of AMPK. These 35 fractions revealed distinct polypeptide band patterns while containing sufficient amounts of proteins and were, therefore, selected for radioactive kinase assays with or without AMPK. Following SDS-PAGE, the labeling of proteins with ^{32}P was then visualized by autoradiography. A crucial step in these assays was to reduce background phosphorylation by endogenous kinases to a minimum while increasing the specific labeling by AMPK. Several strategies to enhance the signal-to-background ratio have been proposed including the application of Mn^{2+} instead of Mg^{2+} as cofactor for the kinase reactions,[39] the use of recombinant kinases mutated in their ATP-binding pocket to allow the exclusive use of ATP analogues,[40] and inactivation of the endogenous kinases by heat treatment or urea.[41,42] Just like many other kinases, AMPK was unable to use [Mn^{2+}]ATP efficiently (results not shown). Custom-made compounds such as N6-(benzyl)-[γ-^{32}P]ATP are very expensive, and engineering of the mutant kinase requires thorough knowledge and subsequent evaluation of its specificity. Heat or urea treatment of the extracts can result in irreversible conformational changes of the kinase substrates that may generate artificial sites of phosphorylation or disrupt existing ones, making this approach less suitable for our purpose. Hence, none of the above strategies was applied in the present study. Instead, prefractionation of the brain extract by serially connected columns and short incubation times (1 min) of the native protein fractions with a large amount of recombinant kinase, as described herein, efficiently reduced background phosphorylation and allowed tracing of new candidate substrates from tissue lysates. An example of such a 1-D screening of Heparin fractions 17−22 is given in Figure 3A. All 35 selected fractions from the prefractionation step were subjected to AMPK-assays, as described above, and screened for potential targets by differential autoradiography. This means that, after comparison of the according lanes on the autoradiographs, only signals appearing exclusively in AMPK-containing lanes were considered to be AMPK-specific. The overall pattern of proteins specifically labeled by AMPK is given in Figure 3B. The potential substrates were distributed well throughout the fractions, with most ^{32}P-signals present in the Heparin elution (Hep) fractions. Although some small redundancies were still observable, many labeled proteins showed a preferential binding to one sorbent. The ^{32}P-signals in the polypeptides obtained with the cation (SP) and anion (Q) exchangers had some similarities in the high molecular weight range but differed substantially below 60 kDa. Even though the Blue-Sepharose (Blue) column, that is expected to capture ATP-binding proteins, was eluted by nucleotides (fractions 1−7) and high concentrations of sodium chloride (fractions 26−30), only two candidate substrates were detected there. The flow-through, that is, all protein species that did not bind to either of the four solid-phase chemistries, contained 10 different putative targets that were specifically phosphorylated by AMPK (Figure 3B, last lane).

2-D Screen for AMPK Substrates. Many different potential substrates of AMPK were detected on the 1-D autoradiographs. However, the assignment of these ^{32}P-signals to the corresponding protein band was ambiguous for two reasons. First, despite prefractionation, the fractions were still of high complexity. This implies that a radioactively labeled gel band is likely to contain more than one polypeptide species after 1-DE,

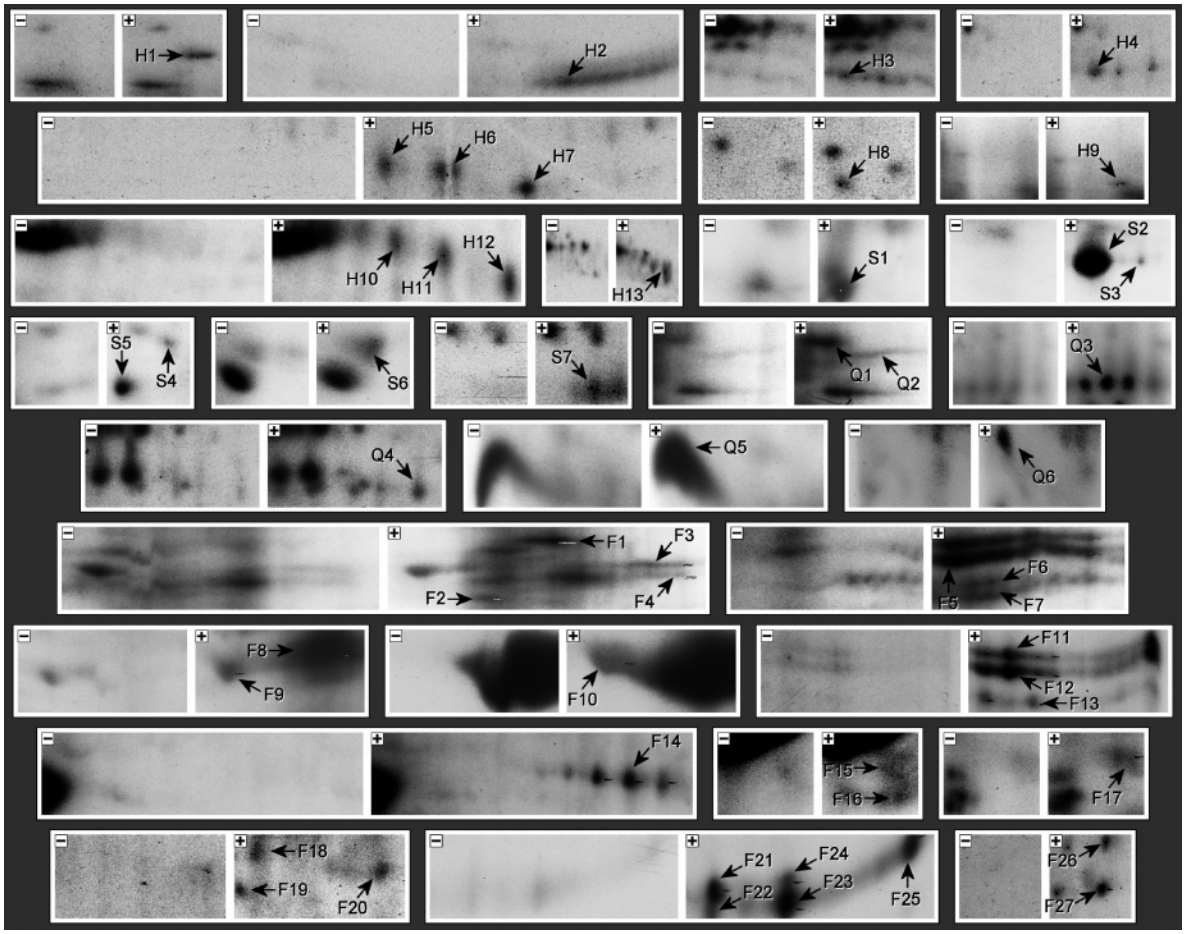

Figure 4. Candidate substrates of AMPK revealed by differential autoradiography after 2-DE. Heparin fractions 19−21 (H1−H13), cation exchanger fraction 20 (S1−S7), anion exchanger fraction 21 (Q1-Q6), and the flow-through (F1−F27) were incubated in the presence of [γ-^{32}P]ATP with recombinant AMPK (+) or without exogenous kinase (-). After protein separation by 2-DE and subsequent gel drying between cellophane sheets, labeling of substrates was detected by autoradiography. A total of 53 signals (black arrows) significantly changed in intensity or emerged newly upon addition of AMPK. These signals were attributed to the corresponding protein spots or areas on the dried gels. A clear assignment was assured by piercing the autoradiography films with a razor blade to mark the appropriate areas on the dried gels (black or white lines in some of the images are consequences thereof). The spots were excised, followed by tryptic in-gel digestion and identification using MALDI mass spectrometry.

thereby leading to a high probability of identification of false-positive targets of AMPK. Second, ^{32}P-signals corresponding to gel areas lacking visible staining of protein bands indicated that these polypeptides were of relatively low abundance. To enhance resolution and increase the protein amount for improved detection, the AMPK-assays were repeated with a subset of fractions at larger scale, this time followed by 2-DE, and then again deploying differential autoradiography. On the basis of the results of the one-dimensional pilot screen (Figure 3B), a subset of four fractions featuring a high diversity in AMPK-specific signals (flow-through (FT), Hep 19, Hep 20, SP 20) were chosen. Additionally, we investigated two fractions in more detail that showed a high endogenous phosphorylation activity (Hep 21 and Q 21), since this could have masked AMPK-labeled candidate substrates. Figure 4 gives an overview of all AMPK-specific ^{32}P-labeled spots that were detected using these six fractions. The position of the radioactive spots on the gels matching the signals on the autoradiograph was accurately determined by refitting the autoradiography films onto the gel and piercing film and subjacent gel at corresponding positions with a razor blade, thereby leaving small scratches in the cellophane layer of the gel. The majority of signals on the autoradiographs clearly matched to corresponding polypeptide spots on the gels. However, a few signals appeared in areas of the gel devoid of visible protein staining, even though a fairly strong radiolabeling was recorded. Such unstained regions were nevertheless excised, as well.

Identification of Downstream Candidate Targets of AMPK. In total, 53 spots were subjected to tryptic in-gel digestion and mass spectrometric analysis (Supporting Information Table S1). As shown in Table 1, 34 protein spots could be identified with a significant probability-based MOWSE score (>63). Solely citrate synthase (CS) was marginally below that statistical threshold with a score of 61.1. Two presumptive candidate targets with an apparent molecular weight of 63 kDa (spots S5 and F8) were identified as AMPK-α1, although these spots were located at unexpected p*I* regions for this subunit. Unlike the β1- and γ1-subunits of AMPK, such imperfect focusing of the catalytic α1-subunit was frequently observed. Another two proteins were identified as the γ1-subunit of AMPK (spots H4 and F21). Most likely, the latter was due to cross-contamination by γ1 that migrated very close to these ^{32}P-labeled proteins, since the γ1 subunit was not found to be phosphorylated *in vivo*.[43] In a few cases, the same proteins were identified from

Table 1. Putative AMPK Substrates Identified with a Significant Score from Six 2-D Gels

description	accession no.	fraction	spot	score[a]	stoichiometry[b]
5′-AMP-activated protein kinase, catalytic alpha-1 chain (AMPK alpha 1)	Q3TUQ7	SP 2	S5	63.4	-
	Q5EG47	FT	F8	250	
5′-AMP-activated protein kinase, gamma-1 subunit (AMPK gamma 1)	O54950	Hep 19	H4	182	-
	O54950	FT	F21	275	
Actin, gamma, cytoplasmic	Q3TSB7	FT	F17	228	{0.93}
ATPase, H+ transporting, lysosomal V1 subunit A	Q8CHX2	FT	F7	198	N.d.
β-Synuclein	Q91ZZ3	Q 21	Q6	289	0.06
Bis(5′-nucleosyl)-tetraphosphatase (Ap4A hydrolase)	P56380	Hep 19	H8	225	N.d.
Citrate synthase, mitochondrial precursor	Q9CZU6	FT	F20	61.1	0.14
Dihydropyrimidinase-like 2 (CRMP2, DRP-2)	Q6P5D0	Hep 21	H13	208	1.12
Dynein intermediate chain 2	O88487	SP 20	S4	128	N.d.
Elongation factor Ts (EF-Ts)	Q9CZR8	Hep 19	H5	118	N.d.
	Q3TA37	Hep 20	H12	79.6	
Elongation factor Tu, mitochondrial precursor	Q8BFR5	FT	F18	201	N.d.
Far upstream element binding protein 1 (FUSE binding protein 1)	Q3TUE1	FT	F13	99	N.d.
Fascin homologue 1 (Fscn1)	Q7TN32	Hep 19	H3	93	N.d.
Glial fibrillary acidic protein (GFAP)	Q3USS4	FT	F15	369	1.84
Glutamate dehydrogenase 1, mitochondrial precursor	P26443	FT	F14	173	0.68
Glutamine synthetase (glutamate-ammonia ligase)	Q91VC6	FT	F19	388	0.21
Glyceraldehyde-3-phosphate dehydrogenase (GAPDH)	UPI0000024B9B	FT	F22	121	0.35
	UPI0000024B9B	FT	F23	220	
	UPI0000563BDB	FT	F25	281	
Heat shock protein 8 (Hspa8, Hsc70, Hsc71)	Q6NZD0	FT	F6	215	×
Heterogeneous nuclear ribonucleoproteins A2/B1 (hnRNP A2/B1)	O88569	FT	F24	132	N.d.
Neurofilament, light polypeptide (neurofilament triplet L protein)	Q8K0Z0	FT	F9	247	N.d.
Ngg1 interacting factor 3-like 1 (NIF3-like protein 1)	Q9EQ80	Q 21	Q3	299	N.d.
NmrA-like family domain containing 1	Q8K2T1	Hep 19	H6	96.1	N.d.
Nucleolin	Q99K50	SP 2	S2	74	N.d.
Protein kinase C and casein kinase substrate in neurons protein 1 (PACSIN1)	Q61644	SP 2	S6	130	0.16
Synapsin-1 (Syn1)	O88935	FT	F5	91.1	5.46
	O88935	FT	F12	78.2	
Telomerase-binding protein p23 (prostaglandin E synthase 3, Hsp90 co-chaperone)	Q9R0Q7	Q 21	Q5	190	0.46
Tripeptidyl-peptidase 2 (TPP 2)	Q64514	Q 21	Q2	161	×
Tubulin, beta 2	Q3TG26	FT	F2	69.4	{1.93}
	Q99JZ6	FT	F10	176	

[a] Probability-based MOWSE score.[35] [b] Stoichiometry of target protein phosphorylation by AMPK expressed as moles phosphate incorporated per mole protein after 2 h of incubation. N.d., not determined; ×, purified protein was not phosphorylated by AMPK *in vitro*; Brackets mean that the tested protein comprised a mixture of isoforms.

different spots on distinct gels or even on the same gel, for example, elongation factor-Ts, tubulin β2, synapsin 1, and glyceraldehyde-3-phosphate dehydrogenase (GAPDH). Interestingly, GAPDH was identified as a potential AMPK substrate in the flow-through (Figure 4, spots F22, F23, and F25), even though no obvious changes in its radioactive labeling were observed after AMPK-assays with the whole brain lysate (Figure 1B, compare intensity of spots 3A and 3B). Presumably, the AMPK-specific labeling of GAPDH was masked due to the actions of endogenous kinases in the total extract or, alternatively, reversed by phosphatase activities, therefore emphasizing the important role of prefractionation. In summary, excluding the proteins identified as AMPK subunits, we found 26 unique potential downstream targets of this kinase.

The fact that all of the identified polypeptides are novel candidate substrates of AMPK, with none of the already known downstream targets being identified in the present screening, may appear unexpected at first glance. However, although the resolving power of 2-DE is unparalleled, this technique entails that some kinase substrates may not be detected and identified. In particular, proteins with large (>200 kDa) and very small (<15 kDa) molecular mass or extreme p*I* (<4, >9) are hardly resolved.[44,45] In addition, solubilization of membrane proteins in the sample buffer is usually insufficient, resulting in a significant underrepresentation of such protein species.[46] These technical limitations may explain, to some extent, the encountered problem of identifying any known AMPK substrates in our study, such as the transmembrane proteins CFTR, the $GABA_B$-receptor, HMG-CoA reductase, or proteins with a high molecular weight like ACC1/ACC2 (both >260 kDa), TSC2 (200 kDa), or AS160 (147 kDa). Moreover, this study represents the first proteome-wide screening for AMPK substrates in brain, whereas most of the previously known targets were discovered based on educated guess. Importantly, while the latter were found in tissues other than brain,[14,47] one-third of the newly identified candidate targets, synapsin-1,[48] collapsing response mediator protein-2 (CRMP-2),[49] protein kinase C, and casein kinase substrate in neurons 1 (PACSIN1),[50] β-synuclein,[51] tubulin β2,[52] neurofilament triplet L protein (NF-L),[53] glial fibrillary acidic protein (GFAP),[54] and glutamine synthetase (GS),[55] are exclusively or predominantly expressed in brain. Conversely, some of the known AMPK targets, for example, carbohydrate responsive element-binding protein,[56] acetyl-CoA carboxylase 2/β,[57] or hormone-sensitive lipase,[58] are poorly expressed in brain compared to other organs and tissues.

***In Vitro* Verification of Identified Candidate Targets.** The wide-range IPG strips (pH 3−10) together with second dimension SDS-PAGE, as used in the screening procedure, sufficiently separated proteins according to p*I* and molecular weight, such that a fair number of candidate target proteins were identified by mass spectrometry. However, to verify direct phosphorylation by AMPK, defined kinase assays with highly purified candidate substrates were mandatory for several reasons. On the one hand, multiple proteins per spot may be present, and cross-contamination of single spots by other protein species remains possible,[33] which would lead to the identification of

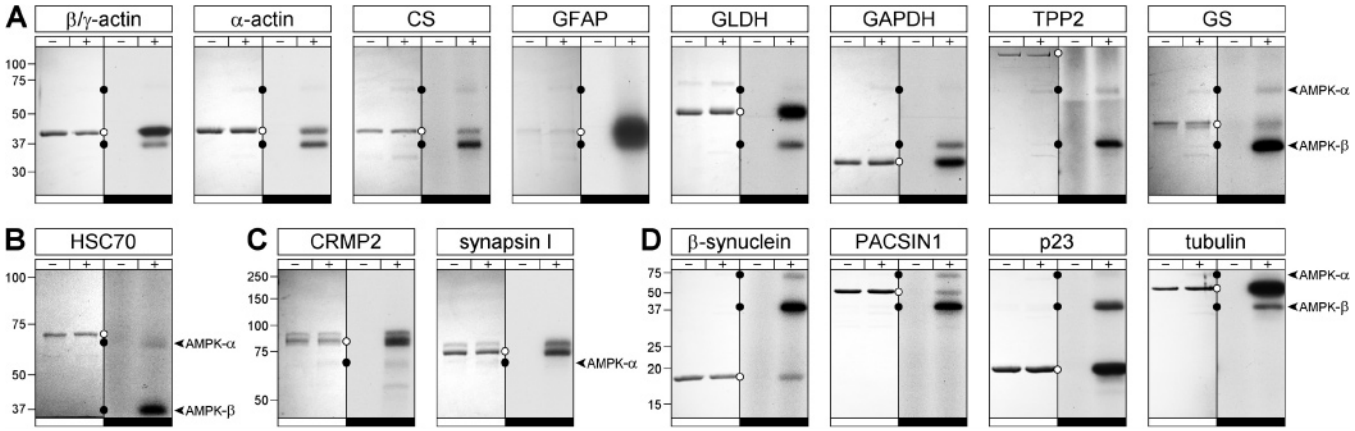

Figure 5. Verification of putative substrates as *in vitro* targets of AMPK. Highly purified candidate targets were incubated with [γ-^{32}P]-ATP in the presence (+) or absence (-) of AMPK. After incubation, reaction mixtures were analyzed by SDS-PAGE and Coomassie Blue-staining. Dried gels were exposed to X-ray sensitive films. For each candidate protein, the Coomassie Blue-stained gel (left, open bars) and the autoradiograph (right, filled bars) are shown. The AMPK α- and β-subunits produce signals derived from autophosphorylation that are marked by filled circles (●), whereas the position of candidate targets is marked by open circles (○). The characteristic of the separating gel was chosen depending on the molecular weight of the target protein: (A) 12%, (B) 8%, (C) 10%, and (D) 15%. Except for two proteins, HSC70 and TPP2, all others were directly phosphorylated by AMPK.

false-positive AMPK targets. On the other hand, a seemingly AMPK-specific incorporation of ^{32}P might also be mediated indirectly, for example, by phosphorylation and activation of an upstream kinase of the putative substrate that coeluted in a particular fraction. Consequently, a subset of 14 candidate proteins was obtained from various sources, and each protein was incubated with [γ-^{32}P]ATP in the presence or absence of recombinant AMPK *in vitro*. Following SDS-PAGE, autoradiography was used to confirm incorporation of radioactive phosphate. As shown in Figure 5, 12 candidate substrates were directly phosphorylated by AMPK *in vitro*. These were actin, tubulin, synapsin I, β-synuclein, prostaglandin E2 synthase (p23), glutamate dehydrogenase (GLDH), GAPDH, GS, CS, GFAP, CRMP2, and PACSIN1. A mixture of α- and β-tubulin was used for verification, leaving open the possibilities that only one or both tubulin isoforms were targeted by AMPK. Likewise, phosphorylation of actin was corroborated using a mixture of β- and γ-isoforms, although only γ-actin was identified by mass spectrometry with a significant score (Table 1). Additionally, α-actin was targeted by AMPK *in vitro* (Figure 5), suggesting that phosphorylation by AMPK is not restricted to a certain actin-isoform. Two candidate proteins, namely, tripeptidyl peptidase II (TPP2) and heat shock cognate 70 (HSC70), were not labeled by AMPK *in vitro*, inconsistent with being a target and rather ruling out direct phosphorylation by AMPK. As shown in Figure 5, the positively verified candidate targets incorporated phosphate to a various extent, as reflected by the varying ^{32}P-signals observed with different targets in comparison with the β1-derived autophosphorylation signal that is presumed to be constant in all incubations. Phosphate incorporation was quantified for each of the targets, and results are listed in Table 1. Overall, the MudSeeK approach delivered a fair number of potential targets, and only a small fraction were false positives, as revealed by *in vitro* phosphorylation with highly purified proteins.

In this study, a heterotrimeric AMPK complex containing the catalytic α1-subunit was used to screen for downstream targets. It was reported that AMPK-α1 and -α2 may behave significantly different concerning its function and regulation *in vivo*.[26] Most probably, such diversity arises from varying expression patterns of all AMPK subunit isoforms in the different regions and cell types of brain,[20] but not from distinct substrate preferences of the two α-subunit isoforms as the latter exhibit only slight differences in the phosphorylation of synthetic peptides.[59] Accordingly, incubation of positively verified candidate targets with AMPK-α2 heterotrimers *in vitro* revealed no significant differences in target protein phosphorylation compared to α1-containing AMPK complexes (Supporting Information Figure S1).

Definitely, the positively verified *in vitro* targets cannot be simply regarded as *bona fide* substrates of AMPK in living organisms. Rather, each of these targets will still need thorough *in vivo* examination to corroborate the findings in the context of the cell, which is, however, going well beyond the scope of this work. Despite these words of caution, considering that AMPK functions in maintaining intracellular ATP levels, some of the potential targets presented here are attractive candidates for being regulated by this kinase. GAPDH, CS, and GLDH are important enzymes in energy-producing pathways such as glycolysis and the tricarboxylic acid (TCA) cycle. Indeed, the brain is a highly energy-consuming organ and utilizes 50% of total body glucose.[60] Although the TCA cycle has the potential to generate much more ATP per mole of glucose than produced by glycolysis, it is believed that the latter process is primarily responsible to meet the increased energy demands during times of high activity in brain.[61,62] Thus, GAPDH is emerging as a reasonable target of AMPK. While GLDH oxidizes glutamate to α-ketoglutarate, which is then metabolized in the TCA cycle to produce reduction equivalents for the regeneration of ATP,[63] CS is crucial in the TCA cycle, catalyzing the production of citrate from acetyl-CoA and oxaloacetate. However, it is believed that both, GLDH and CS, locate exclusively to mitochondria,[64,65] where they presumably would be protected from phosphorylation by AMPK, leaving open the possibility that mitochondrial import of these enzymes could be regulated, that is, stimulated, by AMPK. Indeed, regulation of mitochondrial import by phosphorylation has been shown for several proteins and is increasingly gaining interest.[66−69] Increased neuronal activity, that is, elevated energy turnover in brain, is known to occur during physical exercise[70] and, therefore, likely activates

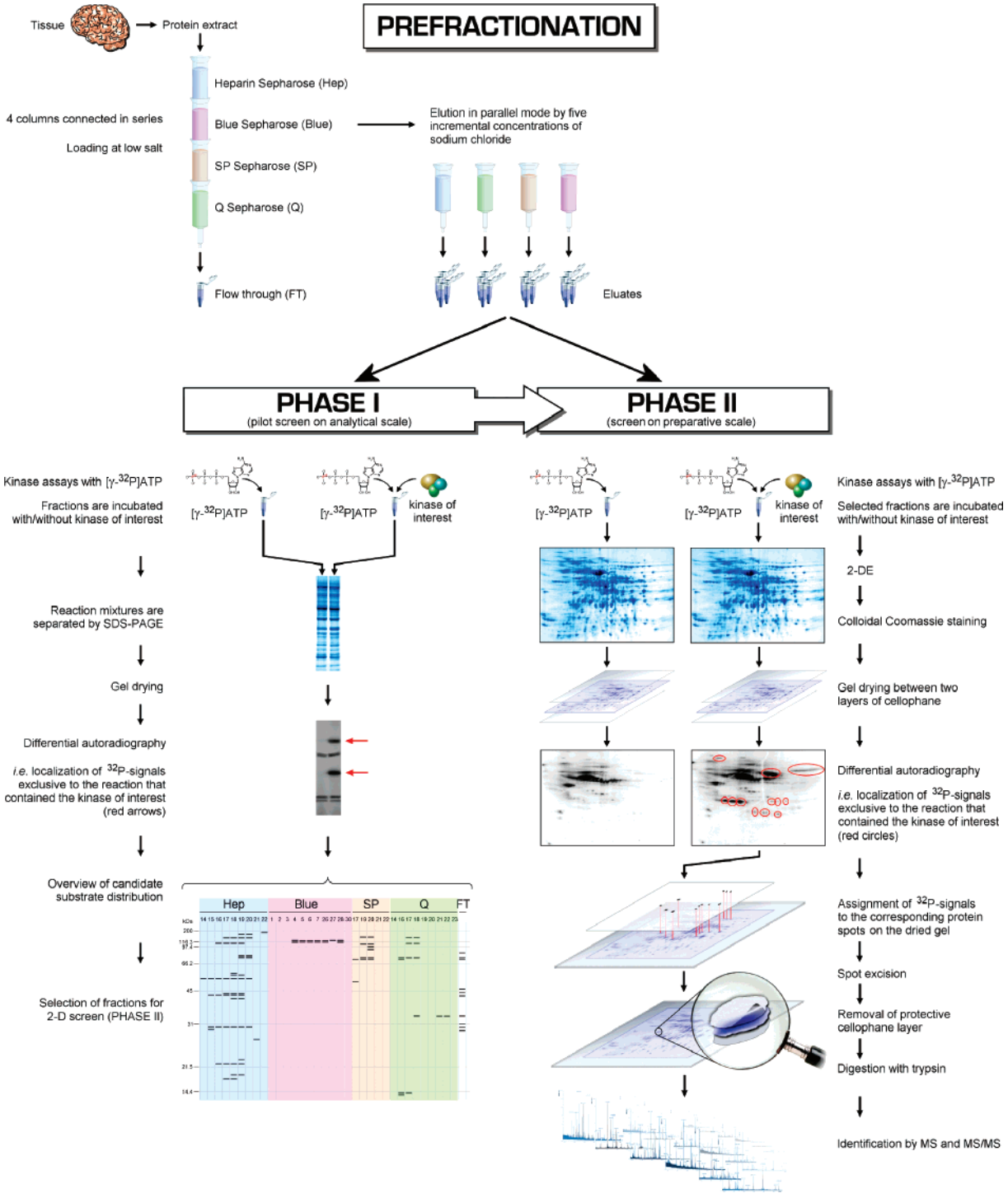

Figure 6. Overview of the MudSeek approach. A tissue-derived protein extract is prefractionated by four serially connected columns with different sorbent chemistries. Each fraction is then analyzed for the presence of potential downstream targets of a given protein kinase involving separation by 1-DE (phase I). Promising fractions are selected for a second screen but on preparative scale and involving separation by 2-DE (phase II), allowing for subsequent spot excision and protein identification by mass spectrometry.

AMPK in brain. Interestingly, it was shown that exercise up-regulates proteins in rat brain that are involved in energy metabolism, such as GLDH,[71] suggesting a physiological link between this enzyme and AMPK. Moreover, the same study revealed that phosphorylation of the cytoskeletal proteins β-tubulin and GFAP, both *in vitro* targets of AMPK (Figure 5), was significantly increased in brain after exercise. Furthermore, phosphorylation of another AMPK candidate target protein listed in Table 1, NF-L, was augmented after exercise.[71] Thus, the data suggest a possible regulatory role of AMPK in brain involving pathways of energy metabolism and cytoskeletal rearrangement that have not been linked to this enzyme yet. In particular, our new findings that actin, tubulin, and GFAP are also likely to be downstream targets of AMPK, would make sense insofar as cell motility and changes in cell structure, as well as the maintenance of polar cell shapes, are highly energy

consuming processes. Thus, one could surmise that, under cellular energy stress, AMPK would lead to a decrease in cytoskeletal dynamics, such as tread milling and polymerization and, thus, would spare the cell from excessive energy expenditure. In support of this, convincing evidence for an energy-dependent regulation of cell structure by AMPK has recently been published.[72]

Apart from being activated by elevated energy demands causing a raise of the intracellular AMP/ATP ratio, stimuli and conditions that do not seem to change AMP levels, such as hyperosmotic stress, were also described to activate AMPK.[16] Hyperosmotic stress is known to raise intracellular calcium levels,[73] and contrary to LKB1, with CaMKKβ being a Ca^{2+}-activated kinase predominantly expressed in brain,[74,75] it is rather expected that AMPK signaling in this organ involves pathways distinct from those established in peripheral tissues. With regard to neurons, phosphorylation of synapsin I by AMPK may affect synaptic vesicle transport and release of neurotransmitters as described for other kinases of synapsin.[76−78] Thus, it is reasonable to speculate that, upon energy shortage, phosphorylation of synapsin by AMPK may shut down further excitation of nerve terminals, thereby preventing energy drain and displaying a neuroprotective function, similar to phosphorylation of the $GABA_B$-receptor as proposed recently.[12] By phosphorylating PACSIN1, a protein responsible for endocytosis of certain *N*-methyl-D-aspartate (NMDA) receptors,[79] AMPK may participate in the synaptic removal of receptors. In contrast to astrocytes, neurons lack glutamine synthetase,[80] an enzyme involved in the ATP-dependent conversion of the neurotransmitter glutamic acid to the non-neuroactive compound glutamine. Indeed, by stopping this reaction through AMPK, glutamic acid would not be diverted to glutamine but would be available to GIDH to feed the TCA cycle for energy production. Hence, the functions of AMPK may not only be tissue-specific, but also dependent on the neuronal cell type.

Again, each of the candidate targets needs evaluation and clarification in terms of involvement of AMPK and physiological relevance *in vivo*. However, we can presume regulation of several energy-related pathways in brain where AMPK is very likely involved. By utilization of the MudSeeK method, we discovered *in vitro* targets of AMPK that are representing good starting points for further studies and that should definitively be taken into account when investigating signaling of AMPK in brain.

Conclusions

Here, we report the first proteome-wide search for potential AMPK substrates using tissue lysates. A prerequisite for our studies was the development of a novel multidimensional screening approach to search for kinase substrates termed MudSeeK (Figure 6). The method proved an effective tool for identification of hitherto unknown potential downstream targets of AMPK with a considerably low number of false-positive hits. Similar to other proteomic analyses, the prefractionation strategy was instrumental for successful application of the screening method, and chromatography by serially stacked sorbents turned out to be a very convenient approach for separation. A sole precondition of the MudSeeK technology is the availability of the protein kinase of interest in an active and purified form, but no further significant restrictions apply. Thus, we can expect universal applicability of the MudSeeK technology for identification of putative downstream targets of any protein kinase from any tissue. Unlike other techniques, pre-existing knowledge concerning the biology or function of the kinase is not required. Merely, the kinase of interest should be expressed in the tissue of study.

By the use of classical ^{32}P-labeling for visualization of kinase-specific substrates, the MudSeek approach was capable of revealing candidate substrates of AMPK in brain. A novel physiological AMPK target, thyroid receptor interacting protein 6, was recently identified by a search for proteins that interact with the α2-subunit of AMPK using yeast two-hybrid (Y2H) screening of a human pancreas cDNA library.[13] While it would be interesting to compare our data set with these Y2H results, because any overlap in the target lists may strongly suggest physiological relevance for such AMPK substrates, the identities of the Y2H positive clones remain unpublished so far. In summary, our findings potentially provide new insights into the functions of AMPK in brain by offering candidate proteins that are likely to be regulated also *in vivo* and are linked with new paradigms. With some of these substrates being present in other tissues as well, the multi-faceted role of AMPK at the whole body level is expected to get innovative physiological clues.

Abbreviations: 2-DE, two-dimensional electrophoresis; ACN, acetonitrile; AMPK, AMP-activated protein kinase; CAMKK, Ca^{2+}/calmodulin-activated protein kinase; CRMP2, collapsin response mediator protein-2; CS, citrate synthase; GAPDH, glyceraldehyde-3-phosphate dehydrogenase; GFAP, glial fibrillary acidic protein; GS, glutamine synthetase; Hsc70, heat shock cognate 70; MudSeek, multidimensional substrate-screen for kinases; NF-L, neurofilament triplet L protein; p23, prostaglandin E2 synthase; PACSIN1, protein kinase C and casein kinase substrate in neurons 1; T2DM, type-2 diabetes mellitus; TCA, tricarboxylic acid; TFA, trifluoracetic acid; TPP2, tripeptidyl peptidase II; Y2H, yeast two-hybrid.

Acknowledgment. We are grateful to R. Scholz for critical reading of this manuscript and to David Toft, Hiroki Morizono, Markus Plomann, and Angus Nairn for kindly providing purified proteins. This work was funded by graduate student stipends from the ETH (to T.W., R.D.T. and R.F.T.), by Swiss National Science Foundation Grant No. 3100AO-114137 (to T.W. and D.N.), by the Helmut-Horten Foundation (to T.W. and D.N), and the FP-6 EU framework programme project No. LSHM-CT-2004-005272 EXGENESIS.

Supporting Information Available: Fifty-seven spots from various 2-D gels were analyzed by mass spectrometry. Four proteins were identified from 2-D gels of total brain lysate, whereas 53 proteins were identified after three-dimensional separation of the murine brain extract. A comprehensive list of these proteins including redundant and ambiguous hits is provided as Supporting Information Table S1. Peptide mass fingerprint and MS/MS data for each of these proteins are given in Supporting Information Tables S2 and S3, respectively. Methods and results of the candidate target verification assays with α2-AMPK are given in Supporting Figure S1. This material is available free of charge via the Internet at http://pubs.acs.org.

References

(1) Hardie, D. G.; Hawley, S. A. AMP-activated protein kinase: the energy charge hypothesis revisited. *BioEssays* **2001**, *23* (12), 1112−9.
(2) Hardie, D. G. The AMP-activated protein kinase pathway−new players upstream and downstream. *J. Cell Sci.* **2004**, *117* (Pt 23), 5479−87.

(3) Hawley, S. A.; Pan, D. A.; Mustard, K. J.; Ross, L.; Bain, J.; Edelman, A. M.; Frenguelli, B. G.; Hardie, D. G. Calmodulin-dependent protein kinase kinase-beta is an alternative upstream kinase for AMP-activated protein kinase. *Cell Metab.* **2005**, *2* (1), 9−19.
(4) Woods, A.; Dickerson, K.; Heath, R.; Hong, S. P.; Momcilovic, M.; Johnstone, S. R.; Carlson, M.; Carling, D. Ca2+/calmodulin-dependent protein kinase kinase-beta acts upstream of AMP-activated protein kinase in mammalian cells. *Cell Metab.* **2005**, *2* (1), 21−33.
(5) Hawley, S. A.; Boudeau, J.; Reid, J. L.; Mustard, K. J.; Udd, L.; Makela, T. P.; Alessi, D. R.; Hardie, D. G. Complexes between the LKB1 tumor suppressor, STRAD alpha/beta and MO25 alpha/beta are upstream kinases in the AMP-activated protein kinase cascade. *J. Biol.* **2003**, *2* (4), 28.
(6) Woods, A.; Johnstone, S. R.; Dickerson, K.; Leiper, F. C.; Fryer, L. G.; Neumann, D.; Schlattner, U.; Wallimann, T.; Carlson, M.; Carling, D. LKB1 is the upstream kinase in the AMP-activated protein kinase cascade. *Curr. Biol.* **2003**, *13* (22), 2004−8.
(7) Carling, D. The AMP-activated protein kinase cascade−a unifying system for energy control. *Trends Biochem. Sci.* **2004**, *29* (1), 18−24.
(8) Corton, J. M.; Gillespie, J. G.; Hardie, D. G. Role of the AMP-activated protein kinase in the cellular stress response. *Curr. Biol.* **1994**, *4* (4), 315−24.
(9) Hardie, D. G.; Hawley, S. A.; Scott, J. W. AMP-activated protein kinase−development of the energy sensor concept. *J. Physiol.* **2006**, *574* (Pt 1), 7−15.
(10) Browne, G. J.; Finn, S. G.; Proud, C. G. Stimulation of the AMP-activated protein kinase leads to activation of eukaryotic elongation factor 2 kinase and to its phosphorylation at a novel site, serine 398. *J. Biol. Chem.* **2004**, *279* (13), 12220−31.
(11) Inoue, E.; Yamauchi, J. AMP-activated protein kinase regulates PEPCK gene expression by direct phosphorylation of a novel zinc finger transcription factor. *Biochem. Biophys. Res. Commun.* **2006**, *351* (4), 793−9.
(12) Kuramoto, N.; Wilkins, M. E.; Fairfax, B. P.; Revilla-Sanchez, R.; Terunuma, M.; Tamaki, K.; Iemata, M.; Warren, N.; Couve, A.; Calver, A.; Horvath, Z.; Freeman, K.; Carling, D.; Huang, L.; Gonzales, C.; Cooper, E.; Smart, T. G.; Pangalos, M. N.; Moss, S. J. Phospho-dependent functional modulation of GABA(B) receptors by the metabolic sensor AMP-dependent protein kinase. *Neuron* **2007**, *53* (2), 233−47.
(13) Solaz-Fuster, M. C.; Gimeno-Alcaniz, J. V.; Casado, M.; Sanz, P. TRIP6 transcriptional co-activator is a novel substrate of AMP-activated protein kinase. *Cell. Signal.* **2006**, *18* (10), 1702−12.
(14) Towler, M. C.; Hardie, D. G. AMP-activated protein kinase in metabolic control and insulin signaling. *Circ. Res.* **2007**, *100* (3), 328−41.
(15) Treebak, J. T.; Glund, S.; Deshmukh, A.; Klein, D. K.; Long, Y. C.; Jensen, T. E.; Jorgensen, S. B.; Viollet, B.; Andersson, L.; Neumann, D.; Wallimann, T.; Richter, E. A.; Chibalin, A. V.; Zierath, J. R.; Wojtaszewski, J. F. AMPK-mediated AS160 phosphorylation in skeletal muscle is dependent on AMPK catalytic and regulatory subunits. *Diabetes* **2006**, *55* (7), 2051−8.
(16) Fryer, L. G.; Parbu-Patel, A.; Carling, D. The Anti-diabetic drugs rosiglitazone and metformin stimulate AMP-activated protein kinase through distinct signaling pathways. *J. Biol. Chem.* **2002**, *277* (28), 25226−32.
(17) Zhou, G.; Myers, R.; Li, Y.; Chen, Y.; Shen, X.; Fenyk-Melody, J.; Wu, M.; Ventre, J.; Doebber, T.; Fujii, N.; Musi, N.; Hirshman, M. F.; Goodyear, L. J.; Moller, D. E. Role of AMP-activated protein kinase in mechanism of metformin action. *J. Clin. Invest.* **2001**, *108* (8), 1167−74.
(18) Shaw, R. J.; Lamia, K. A.; Vasquez, D.; Koo, S. H.; Bardeesy, N.; Depinho, R. A.; Montminy, M.; Cantley, L. C. The kinase LKB1 mediates glucose homeostasis in liver and therapeutic effects of metformin. *Science* **2005**, *310* (5754), 1642−6.
(19) Daval, M.; Diot-Dupuy, F.; Bazin, R.; Hainault, I.; Viollet, B.; Vaulont, S.; Hajduch, E.; Ferre, P.; Foufelle, F. Anti-lipolytic action of AMP-activated protein kinase in rodent adipocytes. *J. Biol. Chem.* **2005**, *280* (26), 25250−7.
(20) Ramamurthy, S.; Ronnett, G. V. Developing a head for energy sensing: AMP-activated protein kinase as a multifunctional metabolic sensor in the brain. *J. Physiol.* **2006**, *574* (Pt 1), 85−93.
(21) Culmsee, C.; Monnig, J.; Kemp, B. E.; Mattson, M. P. AMP-activated protein kinase is highly expressed in neurons in the developing rat brain and promotes neuronal survival following glucose deprivation. *J. Mol. Neurosci.* **2001**, *17* (1), 45−58.
(22) Turnley, A. M.; Stapleton, D.; Mann, R. J.; Witters, L. A.; Kemp, B. E.; Bartlett, P. F. Cellular distribution and developmental expression of AMP-activated protein kinase isoforms in mouse central nervous system. *J. Neurochem.* **1999**, *72* (4), 1707−16.
(23) Xue, B.; Kahn, B. B. AMPK integrates nutrient and hormonal signals to regulate food intake and energy balance through effects in the hypothalamus and peripheral tissues. *J. Physiol.* **2006**, *574* (Pt 1), 73−83.
(24) Andersson, U.; Filipsson, K.; Abbott, C. R.; Woods, A.; Smith, K.; Bloom, S. R.; Carling, D.; Small, C. J. AMP-activated protein kinase plays a role in the control of food intake. *J. Biol. Chem.* **2004**, *279* (13), 12005−8.
(25) Kola, B.; Hubina, E.; Tucci, S. A.; Kirkham, T. C.; Garcia, E. A.; Mitchell, S. E.; Williams, L. M.; Hawley, S. A.; Hardie, D. G.; Grossman, A. B.; Korbonits, M. Cannabinoids and ghrelin have both central and peripheral metabolic and cardiac effects via AMP-activated protein kinase. *J. Biol. Chem.* **2005**, *280* (26), 25196−201.
(26) Minokoshi, Y.; Alquier, T.; Furukawa, N.; Kim, Y. B.; Lee, A.; Xue, B.; Mu, J.; Foufelle, F.; Ferre, P.; Birnbaum, M. J.; Stuck, B. J.; Kahn, B. B. AMP-kinase regulates food intake by responding to hormonal and nutrient signals in the hypothalamus. *Nature* **2004**, *428* (6982), 569−74.
(27) Garcia-Gil, M.; Pesi, R.; Perna, S.; Allegrini, S.; Giannecchini, M.; Camici, M.; Tozzi, M. G. 5′-aminoimidazole-4-carboxamide riboside induces apoptosis in human neuroblastoma cells. *Neuroscience* **2003**, *117* (4), 811−20.
(28) McCullough, L. D.; Zeng, Z.; Li, H.; Landree, L. E.; McFadden, J.; Ronnett, G. V. Pharmacological inhibition of AMP-activated protein kinase provides neuroprotection in stroke. *J. Biol. Chem.* **2005**, *280* (21), 20493−502.
(29) Neumann, D.; Woods, A.; Carling, D.; Wallimann, T.; Schlattner, U. Mammalian AMP-activated protein kinase: functional, heterotrimeric complexes by co-expression of subunits in Escherichia coli. *Protein Expr. Purif.* **2003**, *30* (2), 230−7.
(30) Listrom, C. D.; Morizono, H.; Rajagopal, B. S.; McCann, M. T.; Tuchman, M.; Allewell, N. M. Expression, purification, and characterization of recombinant human glutamine synthetase. *Biochem. J.* **1997**, *328* (Pt 1), 159−63.
(31) Suter, M.; Riek, U.; Tuerk, R.; Schlattner, U.; Wallimann, T.; Neumann, D. Dissecting the role of 5′-AMP for allosteric stimulation, activation, and deactivation of AMP-activated protein kinase. *J. Biol. Chem.* **2006**, *281* (43), 32207−16.
(32) Neuhoff, V.; Arold, N.; Taube, D.; Ehrhardt, W. Improved staining of proteins in polyacrylamide gels including isoelectric focusing gels with clear background at nanogram sensitivity using Coomassie Brilliant Blue G-250 and R-250. *Electrophoresis* **1988**, *9* (6), 255−62.
(33) Gorg, A.; Obermaier, C.; Boguth, G.; Harder, A.; Scheibe, B.; Wildgruber, R.; Weiss, W. The current state of two-dimensional electrophoresis with immobilized pH gradients. *Electrophoresis* **2000**, *21* (6), 1037−53.
(34) Benvenuti, S.; Cramer, R.; Quinn, C. C.; Bruce, J.; Zvelebil, M.; Corless, S.; Bond, J.; Yang, A.; Hockfield, S.; Burlingame, A. L.; Waterfield, M. D.; Jat, P. S. Differential proteome analysis of replicative senescence in rat embryo fibroblasts. *Mol. Cell. Proteomics* **2002**, *1* (4), 280−92.
(35) Pappin, D. J.; Hojrup, P.; Bleasby, A. J. Rapid identification of proteins by peptide-mass fingerprinting. *Curr. Biol.* **1993**, *3* (6), 327−32.
(36) Woods, A.; Vertommen, D.; Neumann, D.; Turk, R.; Bayliss, J.; Schlattner, U.; Wallimann, T.; Carling, D.; Rider, M. H. Identification of phosphorylation sites in AMP-activated protein kinase (AMPK) for upstream AMPK kinases and study of their roles by site-directed mutagenesis. *J. Biol. Chem.* **2003**, *278* (31), 28434−42.
(37) Banks, R. E.; Dunn, M. J.; Hochstrasser, D. F.; Sanchez, J. C.; Blackstock, W.; Pappin, D. J.; Selby, P. J. Proteomics: new perspectives, new biomedical opportunities. *Lancet* **2000**, *356* (9243), 1749−56.
(38) Pedersen, S. K.; Harry, J. L.; Sebastian, L.; Baker, J.; Traini, M. D.; McCarthy, J. T.; Manoharan, A.; Wilkins, M. R.; Gooley, A. A.; Righetti, P. G.; Packer, N. H.; Williams, K. L.; Herbert, B. R. Unseen proteome: mining below the tip of the iceberg to find low abundance and membrane proteins. *J. Proteome Res.* **2003**, *2* (3), 303−11.
(39) Knebel, A.; Morrice, N.; Cohen, P. A novel method to identify protein kinase substrates: eEF2 kinase is phosphorylated and inhibited by SAPK4/p38delta. *EMBO J.* **2001**, *20* (16), 4360−9.

(40) Shah, K.; Liu, Y.; Deirmengian, C.; Shokat, K. M. Engineering unnatural nucleotide specificity for Rous sarcoma virus tyrosine kinase to uniquely label its direct substrates. *Proc. Natl. Acad. Sci. U.S.A.* **1997**, *94* (8), 3565−70.
(41) Troiani, S.; Uggeri, M.; Moll, J.; Isacchi, A.; Kalisz, H. M.; Rusconi, L.; Valsasina, B. Searching for biomarkers of Aurora-A kinase activity: identification of in vitro substrates through a modified KESTREL approach. *J. Proteome Res.* **2005**, *4* (4), 1296−303.
(42) Barati, M. T.; Rane, M. J.; Klein, J. B.; McLeish, K. R. A proteomic screen identified stress-induced chaperone proteins as targets of Akt phosphorylation in mesangial cells. *J. Proteome Res.* **2006**, *5* (7), 1636−46.
(43) Mitchelhill, K. I.; Michell, B. J.; House, C. M.; Stapleton, D.; Dyck, J.; Gamble, J.; Ullrich, C.; Witters, L. A.; Kemp, B. E. Posttranslational modifications of the 5′-AMP-activated protein kinase beta1 subunit. *J. Biol. Chem.* **1997**, *272* (39), 24475−9.
(44) Gygi, S. P.; Corthals, G. L.; Zhang, Y.; Rochon, Y.; Aebersold, R. Evaluation of two-dimensional gel electrophoresis-based proteome analysis technology. *Proc. Natl. Acad. Sci. U.S.A.* **2000**, *97* (17), 9390−5.
(45) Wu, C. C.; MacCoss, M. J. Shotgun proteomics: tools for the analysis of complex biological systems. *Curr. Opin. Mol. Ther.* **2002**, *4* (3), 242−50.
(46) Santoni, V.; Molloy, M.; Rabilloud, T. Membrane proteins and proteomics: un amour impossible? *Electrophoresis* **2000**, *21* (6), 1054−70.
(47) Kahn, B. B.; Alquier, T.; Carling, D.; Hardie, D. G. AMP-activated protein kinase: ancient energy gauge provides clues to modern understanding of metabolism. *Cell. Metab.* **2005**, *1* (1), 15−25.
(48) De Camilli, P.; Benfenati, F.; Valtorta, F.; Greengard, P. The synapsins. *Annu. Rev. Cell. Biol.* **1990**, *6*, 433−60.
(49) Wang, L. H.; Strittmatter, S. M. A family of rat CRMP genes is differentially expressed in the nervous system. *J. Neurosci.* **1996**, *16* (19), 6197−207.
(50) Plomann, M.; Lange, R.; Vopper, G.; Cremer, H.; Heinlein, U. A.; Scheff, S.; Baldwin, S. A.; Leitges, M.; Cramer, M.; Paulsson, M.; Barthels, D. PACSIN, a brain protein that is upregulated upon differentiation into neuronal cells. *Eur. J. Biochem.* **1998**, *256* (1), 201−11.
(51) Jakes, R.; Spillantini, M. G.; Goedert, M. Identification of two distinct synucleins from human brain. *FEBS Lett.* **1994**, *345* (1), 27−32.
(52) Sullivan, K. F.; Cleveland, D. W. Identification of conserved isotype-defining variable region sequences for four vertebrate beta tubulin polypeptide classes. *Proc. Natl. Acad. Sci. U.S.A.* **1986**, *83* (12), 4327−31.
(53) Coulombe, P. A.; Ma, L.; Yamada, S.; Wawersik, M. Intermediate filaments at a glance. *J. Cell Sci.* **2001**, *114* (Pt 24), 4345−7.
(54) Eng, L. F.; Ghirnikar, R. S.; Lee, Y. L. Glial fibrillary acidic protein: GFAP-thirty-one years (1969−2000). *Neurochem. Res.* **2000**, *25* (9−10), 1439−51.
(55) Zhang, J.; Moseley, A.; Jegga, A. G.; Gupta, A.; Witte, D. P.; Sartor, M.; Medvedovic, M.; Williams, S. S.; Ley-Ebert, C.; Coolen, L. M.; Egnaczyk, G.; Genter, M. B.; Lehman, M.; Lingrel, J.; Maggio, J.; Parysek, L.; Walsh, R.; Xu, M.; Aronow, B. J. Neural system-enriched gene expression: relationship to biological pathways and neurological diseases. *Physiol. Genomics* **2004**, *18* (2), 167−83.
(56) Iizuka, K.; Bruick, R. K.; Liang, G.; Horton, J. D.; Uyeda, K. Deficiency of carbohydrate response element-binding protein (ChREBP) reduces lipogenesis as well as glycolysis. *Proc. Natl. Acad. Sci. U.S.A.* **2004**, *101* (19), 7281−6.
(57) Abu-Elheiga, L.; Almarza-Ortega, D. B.; Baldini, A.; Wakil, S. J. Human acetyl-CoA carboxylase 2. Molecular cloning, characterization, chromosomal mapping, and evidence for two isoforms. *J. Biol. Chem.* **1997**, *272* (16), 10669−77.
(58) Kraemer, F. B.; Patel, S.; Saedi, M. S.; Sztalryd, C. Detection of hormone-sensitive lipase in various tissues. I. Expression of an HSL/bacterial fusion protein and generation of anti-HSL antibodies. *J. Lipid Res.* **1993**, *34* (4), 663−71.
(59) Woods, A.; Salt, I.; Scott, J.; Hardie, D. G.; Carling, D. The alpha1 and alpha2 isoforms of the AMP-activated protein kinase have similar activities in rat liver but exhibit differences in substrate specificity in vitro. *FEBS Lett.* **1996**, *397* (2−3), 347−51.
(60) Fehm, H. L.; Kern, W.; Peters, A. The selfish brain: competition for energy resources. *Prog. Brain Res.* **2006**, *153*, 129−40.
(61) Magistretti, P. J.; Pellerin, L. Cellular mechanisms of brain energy metabolism. Relevance to functional brain imaging and to neurodegenerative disorders. *Ann. N. Y. Acad. Sci.* **1996**, *777*, 380−7.
(62) Magistretti, P. J.; Pellerin, L. Cellular mechanisms of brain energy metabolism and their relevance to functional brain imaging. *Philos. Trans. R. Soc. London, Ser. B* **1999**, *354* (1387), 1155−63.
(63) Sonnewald, U.; Westergaard, N.; Petersen, S. B.; Unsgard, G.; Schousboe, A. Metabolism of [U-13C]glutamate in astrocytes studied by 13C NMR spectroscopy: incorporation of more label into lactate than into glutamine demonstrates the importance of the tricarboxylic acid cycle. *J. Neurochem.* **1993**, *61* (3), 1179−82.
(64) Fang, J.; Hsu, B. Y.; MacMullen, C. M.; Poncz, M.; Smith, T. J.; Stanley, C. A. Expression, purification and characterization of human glutamate dehydrogenase (GDH) allosteric regulatory mutations. *Biochem. J.* **2002**, *363* (Pt 1), 81−7.
(65) Wiegand, G.; Remington, S. J. Citrate synthase: structure, control, and mechanism. *Annu. Rev. Biophys. Biophys. Chem.* **1986**, *15*, 97−117.
(66) Dasari, V. R.; Anandatheerthavarada, H. K.; Robin, M. A.; Boopathi, E.; Biswas, G.; Fang, J. K.; Nebert, D. W.; Avadhani, N. G. Role of protein kinase C-mediated protein phosphorylation in mitochondrial translocation of mouse CYP1A1, which contains a non-canonical targeting signal. *J. Biol. Chem.* **2006**, *281* (41), 30834−47.
(67) Lee, J.; O'Neill, R. C.; Park, M. W.; Gravel, M.; Braun, P. E. Mitochondrial localization of CNP2 is regulated by phosphorylation of the N-terminal targeting signal by PKC: implications of a mitochondrial function for CNP2 in glial and non-glial cells. *Mol. Cell. Neurosci.* **2006**, *31* (3), 446−62.
(68) Robin, M. A.; Anandatheerthavarada, H. K.; Biswas, G.; Sepuri, N. B.; Gordon, D. M.; Pain, D.; Avadhani, N. G. Bimodal targeting of microsomal CYP2E1 to mitochondria through activation of an N-terminal chimeric signal by cAMP-mediated phosphorylation. *J. Biol. Chem.* **2002**, *277* (43), 40583−93.
(69) Robin, M. A.; Prabu, S. K.; Raza, H.; Anandatheerthavarada, H. K.; Avadhani, N. G. Phosphorylation enhances mitochondrial targeting of GSTA4−4 through increased affinity for binding to cytoplasmic Hsp70. *J. Biol. Chem.* **2003**, *278* (21), 18960−70.
(70) Carro, E.; Nunez, A.; Busiguina, S.; Torres-Aleman, I. Circulating insulin-like growth factor I mediates effects of exercise on the brain. *J. Neurosci.* **2000**, *20* (8), 2926−33.
(71) Ding, Q.; Vaynman, S.; Souda, P.; Whitelegge, J. P.; Gomez-Pinilla, F. Exercise affects energy metabolism and neural plasticity-related proteins in the hippocampus as revealed by proteomic analysis. *Eur. J. Neurosci.* **2006**, *24* (5), 1265−76.
(72) Lee, J. H.; Koh, H.; Kim, M.; Kim, Y.; Lee, S. Y.; Karess, R. E.; Lee, S. H.; Shong, M.; Kim, J. M.; Kim, J.; Chung, J. Energy-dependent regulation of cell structure by AMP-activated protein kinase. *Nature* **2007**, *447* (7147), 1017−20.
(73) Qin, S.; Minami, Y.; Hibi, M.; Kurosaki, T.; Yamamura, H. Syk-dependent and -independent signaling cascades in B cells elicited by osmotic and oxidative stress. *J. Biol. Chem.* **1997**, *272* (4), 2098−103.
(74) Anderson, K. A.; Means, R. L.; Huang, Q. H.; Kemp, B. E.; Goldstein, E. G.; Selbert, M. A.; Edelman, A. M.; Fremeau, R. T.; Means, A. R. Components of a calmodulin-dependent protein kinase cascade. Molecular cloning, functional characterization and cellular localization of Ca2+/calmodulin-dependent protein kinase kinase beta. *J. Biol. Chem.* **1998**, *273* (48), 31880−9.
(75) Kitani, T.; Okuno, S.; Fujisawa, H. Molecular cloning of Ca2+/calmodulin-dependent protein kinase kinase beta. *J. Biochem. (Tokyo)* **1997**, *122* (1), 243−50.
(76) Chi, P.; Greengard, P.; Ryan, T. A. Synaptic vesicle mobilization is regulated by distinct synapsin I phosphorylation pathways at different frequencies. *Neuron* **2003**, *38* (1), 69−78.
(77) Menegon, A.; Bonanomi, D.; Albertinazzi, C.; Lotti, F.; Ferrari, G.; Kao, H. T.; Benfenati, F.; Baldelli, P.; Valtorta, F. Protein kinase A-mediated synapsin I phosphorylation is a central modulator of Ca2+-dependent synaptic activity. *J. Neurosci.* **2006**, *26* (45), 11670−81.
(78) Yamagata, Y. New aspects of neurotransmitter release and exocytosis: dynamic and differential regulation of synapsin I phosphorylation by acute neuronal excitation in vivo. *J. Pharmacol. Sci.* **2003**, *93* (1), 22−9.
(79) Perez-Otano, I.; Lujan, R.; Tavalin, S. J.; Plomann, M.; Modregger, J.; Liu, X. B.; Jones, E. G.; Heinemann, S. F.; Lo, D. C.; Ehlers, M. D. Endocytosis and synaptic removal of NR3A-containing NMDA receptors by PACSIN1/syndapin1. *Nat. Neurosci.* **2006**, *9* (5), 611−21.
(80) Norenberg, M. D.; Martinez-Hernandez, A. Fine structural localization of glutamine synthetase in astrocytes of rat brain. *Brain Res.* **1979**, *161* (2), 303−10.

PR070160A